Influence of emissivity on behavior of metallic dust particles in plasmas

doi: 10.1063/1.2946435

Influence of emissivity on behavior of metallic dust particles in plasmas

Y. Tanaka,[1,a)] R. D. Smirnov,[2] A. Yu. Pigarov,[2] and M. Rosenberg[3]
[1]*Division of Electrical Engineering and Computer Science, Kanazawa University, Kakuma, Kanazawa 920-1192, Japan*
[2]*Department of Mechanical and Aerospace Engineering, University of California at San Diego, La Jolla, California 92093, USA*
[3]*Department of Electrical and Computer Engineering, University of California at San Diego, La Jolla, California 92093, USA*

(Received 15 April 2008; accepted 16 May 2008; published online 15 July 2008)

Influence of thermal radiation emissivity on the lifetime of a dust particle in plasmas is investigated for different fusion relevant metals (Li, Be, Mo, and W). The thermal radiation is one of main cooling mechanisms of the dust in plasmas especially for dust with evaporation temperature higher than 2500 K. In this paper, the temperature- and radius-dependent emissivity of dust particles is calculated using Mie theory and temperature-dependent optical constants for the above metallic materials. The lifetime of a dust particle in uniform plasmas is estimated with the calculated emissivity using the dust transport code DUSTT [A. Pigarov *et al.*, Physics of Plasmas **12**, 122508 (2005)], considering other dust cooling and destruction processes such as physical and chemical sputtering, melting and evaporation, electron emission etc. The use of temperature-dependent emissivity calculated with Mie theory provides a longer lifetime of the refractory metal dust particle compared with that obtained using conventional emissivity constants in the literature. The dynamics of heavy metal dust particles are also presented using the calculated emissivity in a tokamak plasma. © *2008 American Institute of Physics*. [DOI: 10.1063/1.2946435]

I. INTRODUCTION

Recently, the presence of dust in fusion devices attracted much interest among fusion scientists and engineers because it can affect plasma operation and performances in fusion devices. The dust can be an important contributor to impurity contamination of the core and scrape-off-layer plasmas in tokamak fusion devices.[1–4] This impurity contamination may increase radiation energy loss from the plasmas and affect recycling regimes in the divertor regions. Dust also can increase the tritium in-vessel retention and the risk of explosion at an accidental air or coolant leakage, which is important for the safety of fusion devices. Thus, dust has become an important research area for large-scale fusion plasma experiments and numerical simulations to determine the mechanisms of dust production, dust-plasma and dust surface interactions, dust transport, removal, etc.[1–23]

In our previous paper,[24] we estimated the lifetime of dust particles made of the fusion-related materials Li, B, Be, C, Fe, Mo, and W in uniform plasmas using the DUSTT code, and also simulated the behaviors of the dust in the edge plasma of a tokamak. The DUSTT code takes into account various plasma-dust interaction processes including physical and chemical sputtering, radiation enhanced sublimation, melting, and thermal evaporation/sublimation, thermal radiation, as well as dust charging processes such as plasma collection, secondary electron emission, thermionic emission, etc. From the above calculations, we also found that thermal radiation energy loss is one of important processes to cool down dust particles. Since the thermal radiation from the dust also influences the equilibrium temperature for evaporation and thus the evaporation rates, it plays a role in determining the lifetime of the dust particle. The lifetime of the dust in its turn is related to the ability of a dust particle to be an impurity source in the plasma. Therefore, it is important to estimate accurately the power loss from dust thermal radiation, which involves using the temperature- and radius-dependent emissivity of a dust particle for accurate prediction of dust behavior and lifetime in plasmas.

Recently, Rosenberg *et al.* evaluated temperature- and radius-dependent emissivity of a metallic dust particle made of beryllium, stainless steel, molybdenum, and tungsten, for a wide dust radius range of 0.01 to 10 μm, and in a temperature range from 300 K to the dust melting point.[25] They used the Mie theory to calculate light absorption efficiency factor[26,27] and Drude theory to estimate the temperature-dependent optical constants,[28–31] and calculated the total emissivity of the metallic dust particle. As a result, it has been found that the temperature and radius dependences of the emissivity was relatively large, and the emissivity can vary by a factor of more than 100 as a function of dust radius and temperature in a particular case.[25] Their calculation result of the emissivity may also imply large differences in temperature determination of a small particle with a radiation thermometer if one uses a conventional constant emissivity. In addition, such strong temperature and radius dependences of the emissivity can influence prediction on the dynamics and the lifetime of the dust particle in fusion plasmas.

In this paper, first, the optical emissivities calculated by the Mie theory are shown for dust particles made of metals like Be, SUS (stainless steel), Mo, and W as well as Li (see Ref. 32) as functions of dust radius and dust temperature.

[a)]Author to whom correspondence should be addressed. Electronic mail: tanaka@ec.t.kanazawa-u.ac.jp.

Secondly, by using numerical simulations with the dust transport code DUSTT[1] including the calculated temperature- and radius-dependent emissivity, temporal variations in the dust temperature and radius, the thermal radiation energy loss of dust particles were estimated in uniform plasmas with typical parameters for the edge plasma of fusion devices. These variations were compared for dust with three different emissivity models. Thirdly, the dependence of dust survival time on plasma parameters are presented for different metallic materials using newly calculated emissivity. Finally, an example of dust dynamics in the edge plasma of a tokamak is shown to illustrate influence of the emissivity on dust dynamics there.

II. EMISSIVITY OF A DUST PARTICLE

Generally, emissivity ε of a material is defined as the ratio of thermal radiation intensity from the material to the radiation intensity from a black body at the same temperature. The total emissivity of a surface relates its thermal radiation intensity I_{rad} in the whole radiated spectrum to that of a black body and can be written as

$$\varepsilon = \frac{I_{\mathrm{rad}}}{\sigma_{\mathrm{SB}} T^4}, \tag{1}$$

where σ_{SB} is the Stefan-Boltzmann constant and T is the surface temperature. The spectral emissivity is used to describe radiative properties of a body at a given wavelength. According to Kirchoff's law, the spectral emissivity of a dust particle can be given by its absorption efficiency factor Q_{abs}, which defines part of an incident radiation power at a given wave length absorbed by the particle. The absorption efficiency of a small particle depends strongly on the ratio of the particle's size to the wavelength. Generally, the absorption efficiency factor of a dust particle remarkably decreases, when its radius becomes smaller than the radiation wavelength. In addition to the radius dependence, the radiative properties of dust also depend on the temperature due to the temperature dependence of the dust material optical constants. In this paper we consider dust temperature in the range from the room temperature 300 K to the boiling temperature of dust material, which can markedly affect the emissivity. Considering the absorption efficiency factor of the dust particle as a function of the temperature and the radius, the total thermal radiation intensity I_{rad} from a dust particle can be calculated as

$$I_{\mathrm{rad}} = \pi \int_0^\infty Q_{\mathrm{abs}}(T_d, \lambda, r_d) P(T_d, \lambda) d\lambda, \tag{2}$$

where $Q_{\mathrm{abs}}(T_d, \lambda, r_d)$ is the absorption efficiency of a dust particle, which depends on the dust temperature T_d, the wavelength of the light λ, and the dust radius r_d. The radiation spectrum of a black body $P(T_d, \lambda)$ at temperature T_d is given by the Planck function

$$P(T_d, \lambda) = \frac{2c^2 h}{\lambda^5} \frac{1}{\exp\left(\frac{hc}{\lambda k_{\mathrm{B}} T_d}\right) - 1}, \tag{3}$$

where h, c, and k_{B} are, respectively, Planck's constant, the speed of light, and the Boltzmann constant.

However, in studies of dust behavior in plasmas the emissivity dependence on the temperature or/and the radius of the dust particles is often omitted. In this paper, we consider and compare the following three models: Model A, in which the dust emissivity is assumed constant, Model B, which introduces a simple small-body correction to the emissivity, and Model C, which calculates the dust emissivity using the Mie theory taking into account temperature dependence of the dust material optical constants. The models and the corresponding evaluated dust emissivities are described in the next sections.

A. Model A: Constant emissivity

Usually, experimental values of total emissivity of materials are available only for flat surfaces in a narrow temperature range. Such emissivity can be found in the literature,[33] and is often used as a constant value for some applications to bulk metals, for temperature determinations in experiments[34] or numerical simulations of the dust dynamics.[35] For present calculations, we assumed the constant total emissivity to be 0.1 for Li, 0.15 for Be, 0.35 for stainless steel, 0.2 for Mo, and 0.4 for W.[33] However, the adoption of the constant emissivity may lead to significant differences for small particle calculations, because the particle emissivity may have strong size and temperature dependences.

B. Model B: Small-body correction

To consider the dust size effect on the thermal radiation, a small-body correction has been used for the emissivity of a dust particle in the previous work.[3] In this model, the following expression was used, when the dust radius became smaller than a characteristic wavelength of thermal radiation λ_0, viz., for $2\pi r_d |n| / \lambda_0 < 1$,

$$\varepsilon = 8\pi \frac{2\pi}{1.3} \left(\frac{r_d}{\lambda_0(T_d)}\right) \mathrm{Im}\left[\frac{\epsilon - 1}{\epsilon + 2}\right], \tag{4}$$

where ϵ is the complex dielectric function of the dust material, λ_0 is the wavelength of maximum of black-body thermal radiation from the Wien's law (note that $\lambda_0 \propto 1/T_d$), $n = \sqrt{\epsilon}$ is the complex index of refraction of the dust material. Otherwise, a constant emissivity of Model A was used. This model takes into account dependence of the emissivity on the dust radius for small particles. However, it does not account for the temperature dependence of the optical constants that should be considered for a dust particle, whose temperature may vary in a wide range in plasmas.

C. Model C: Using Mie theory

Recently, Rosenberg *et al.* have considered the emissivity of metallic dust particles as function of dust temperature and dust radius using the Mie theory along with a Drude

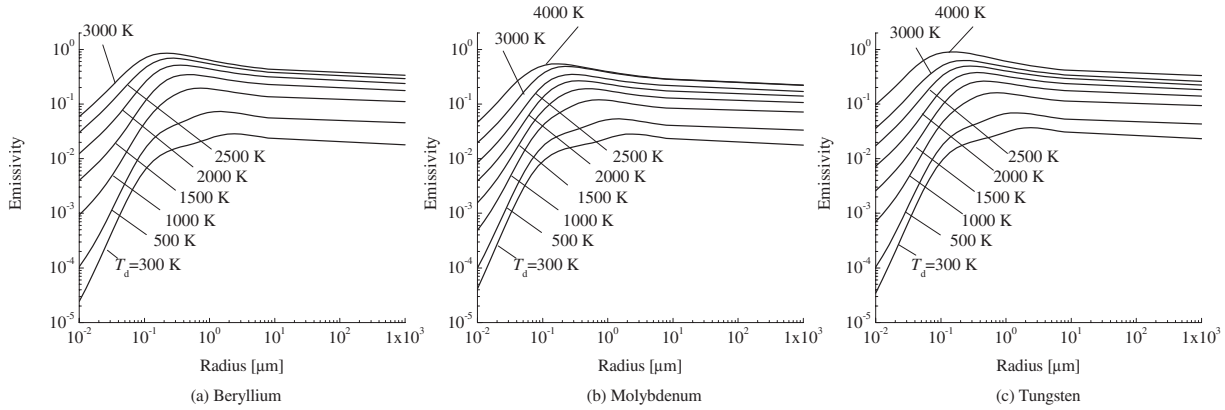

FIG. 1. Emissivity of metallic dust particles as function of dust radius for different dust temperatures as calculated by Mie theory. (a) Beryllium, (b) molybdenum, and (c) tungsten.

theory model for the optical constants.[25] The Mie theory gives an analytic solution of Maxwell's equation for the extinction, i.e., scattering and absorption, of electromagnetic radiation by a sphere. According to this theory, the Q_{abs} can be expressed as multipole series expansion independently for electric and magnetic parts of the absorption (e.g., Ref. 36):

$$Q_{\mathrm{abs}} = \frac{1}{\pi r_d^2}\frac{2\pi}{k^2}\left(\sum_{\nu=1}^{\infty}(2\nu+1)\mathrm{Re}[a_\nu + b_\nu] - \sum_{\nu=1}^{\infty}(2\nu+1)[|a_\nu|^2 + |b_\nu|^2]\right), \tag{5}$$

with

$$a_\nu = \frac{m\psi_\nu(mx)\psi'_\nu(x) - \psi_\nu(x)\psi'_\nu(mx)}{m\psi_\nu(mx)\zeta'_\nu(x) - \zeta_\nu(x)\psi'_\nu(mx)}, \tag{6}$$

and

$$b_\nu = \frac{\psi_\nu(mx)\psi'_\nu(x) - m\psi_\nu(x)\psi'_\nu(mx)}{\psi_\nu(mx)\zeta'_\nu(x) - m\zeta_\nu(x)\psi'_\nu(mx)}, \tag{7}$$

where ψ_ν and ζ_ν are the Riccati-Bessel functions. Here, the relative refractive index m is the ratio of the complex index of refraction of the dust material n to the real index of refraction n_0 of the host medium. The size parameter x is $(2\pi n_0 r_d)/\lambda$ and $k=(2\pi n_0/\lambda)$. For some metals the refraction index can be expressed as a function of the electrical conductivity using Drude theory (see Refs. 29–31). The temperature dependence of DC conductivity σ_{DC} for different metals is available in literatures,[37–39] and the optical conductivity σ_o in frequency range of the thermal radiation (mostly infrared) can be obtained using a correction factor f, so that $\sigma_{\mathrm{DC}}=f\sigma_o$.[29–31,40] Using the conductivity σ_o, we obtain the complex index of refraction of dust material as function of the temperature using the Drude theory, and then calculate Q_{abs} using Mie theory computational code.[41]

For integration of Eq. (2) we used a short wavelength cutoff[25,26] as

$$I_{\mathrm{rad}} = \pi\int_{\lambda_c}^{\infty} Q_{\mathrm{abs}}(T_d,\lambda,r_d)P(T_d,\lambda)d\lambda, \tag{8}$$

where $\lambda_c=4\pi c/\omega_p$, and ω_p is Drude's free electron plasma frequency. This is to avoid errors related to inaccuracy in calculation of the electrical conductivity from Drude theory for the short wavelengths.[25]

Figures 1(a)–1(c) show the calculated total emissivities of beryllium, molybdenum, and tungsten dust particles, respectively, as functions of dust particle radius in range from 0.01 to 1000 μm for different dust temperatures. The emissivities for temperatures until the boiling point were estimated only by extrapolation, when there are no data on electrical conductivity. The figures demonstrate a strong dependence of the emissivity on the dust radius, especially for dust radii below 1.0 μm in the dust temperature range considered. For example, at the temperature of 300 K, the emissivity of tungsten is about 2×10^{-2} for a dust radius of 1.0 μm. If the dust radius is reduced from 1.0 to 0.01 μm, the emissivity is decreased from 2×10^{-2} to about 4×10^{-5}. The large decrease in the emissivity occurs due to decreasing dust absorption efficiency factor, where the dust radius becomes smaller than the wavelengths of the maximum of the black-body radiation at given temperature. Note that for temperatures below 1000 K the emissivity has a more sharp dependence on the radius. This is due to prevalence of the magnetic dipole component of the absorption efficiency factor for highly conductive metals at the low temperatures, which is proportional to the dust radius cubed.[25,42] For the temperatures above 2000 K, the electric dipole component can dominate in the absorption efficiency since the dust material becomes less conductive. That causes more gradual decrease of the emissivity with the dust radius at the high temperatures, because the electric dipole absorption efficiency is proportional to the radius.

On the other hand, the emissivity decreases gradually, when the dust radius increases from 1.0 to 1000 μm. This gradual decrease in the emissivity versus increasing radius is attributed to the fact that the diffraction effect becomes smaller for larger dust particles. In addition to the radius dependence, a strong temperature dependence can be seen in

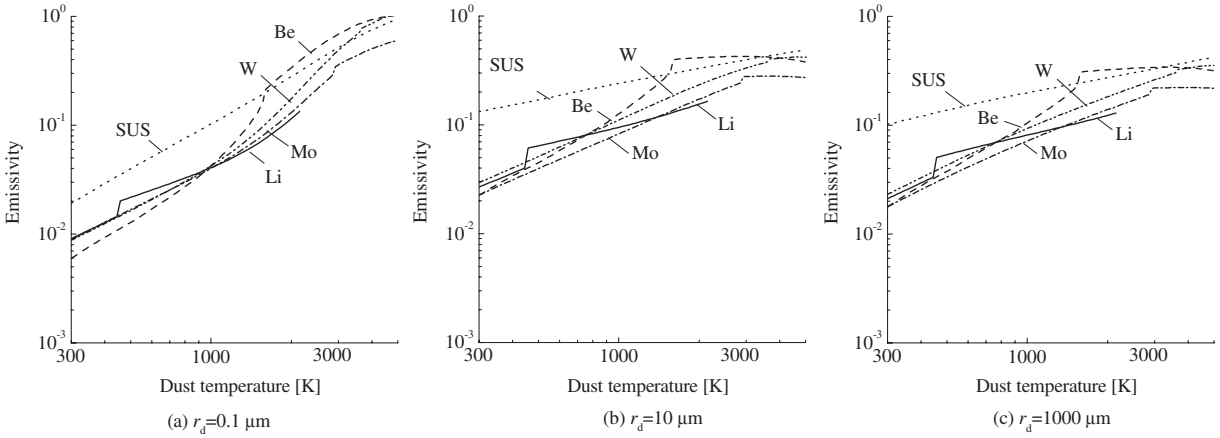

FIG. 2. Emissivity of different metallic dust particles calculated by Mie theory. (a) Dust radius r_d=0.1 μm, (b) r_d=10 μm, (c) r_d=1000 μm.

the emissivity especially for small particles. This temperature dependence of the emissivity results from the temperature dependence of the optical constants, which are related to the electrical conductivity of the dust material (e.g., Ref. 25). The character of the dependence of the emissivity on temperature was found to be similar for the metals considered, as seen in Fig. 1.

Figures 2(a)–2(c) depict the calculated emissivity for a dust particle made of different materials as a function of dust temperature at different radii of 10^{-1}, 10^{1}, and 10^{3} μm. In these figures, there is a stepped change in the emissivity curves of Li, Be, and Mo dust particles. The stepped change in the emissivity curve is due to a stepped change in the electrical conductivity between solid and molten states for materials of Li, Be, and Mo, as discussed in Ref. 32. Again, differences in the emissivity of the considered materials result from differences in the electrical conductivity through their optical constant.

III. ESTIMATION OF THE LIFETIME OF METALLIC DUST PARTICLE IN A UNIFORM PLASMA WITH THE DUSTT CODE

A. The DUSTT code

We used the DUSTT code[1,3] to calculate dust lifetimes in tokamak plasmas. Details of underlying physics and modelling in the DUSTT code are available in the previous references. The DUSTT code simulates three dimensional dynamics of individual dust particles in the edge plasmas, incorporating plasma parameters calculated with the UEDGE code.[9]

The main improvement introduced in this paper for the DUSTT code is that the temperature- and radius-dependent emissivity $\varepsilon(T_d, r_d)$ described in the previous section was used to evaluate total thermal radiation loss as

$$P_{\text{rad}} = 4\pi r_d^2 \varepsilon(T_d, r_d)\sigma_{\text{SB}}(T_d^4 - T_w^4), \tag{9}$$

where T_d is the dust temperature, and T_w is the chamber wall temperature. The temperature- and radius-dependent emissivity can affect the temperature variation of a dust particle especially if it is composed of a material with higher evaporation/sublimation temperatures; this can affect the evaporation rate and the lifetime of the dust particle.

IV. LIFETIME OF DUST PARTICLES IN UNIFORM PLASMAS

A. Calculation conditions

Using the calculated emissivity, the lifetime of a dust particle in uniform plasmas was estimated for different dust materials. For this study, the values of plasma parameters were selected as follows: $T_i = T_e$, $T_a = 0.3T_i$, $n_e = n_i = n_a$, $|\mathbf{E}| = 0$, $|\mathbf{g}| = 0$, where T_i, T_e, and T_a are, respectively, the temperatures of ions, electrons, and neutral atoms, and n_i, n_e, and n_a are the density of ions, electrons, and neutral atoms, respectively. The background plasma is assumed to be a deuterium plasma without any impurities. In this case there is no deposition of plasma impurities onto the dust during travelling in the plasma. The ion flow velocity was set at 10% of the ion sound speed, i.e., $v_i = 0.1\sqrt{(T_i + T_e)/m_i}$, whereas dust particles were assumed immobile in the laboratory system of coordinates. As seen in the previous section, we used the three models for the emissivity for comparison: the constant emissivity used widely for many application works (Model A), the emissivity using small-body correction (Model B), and the emissivity using the full Mie theory (Model C) with the temperature-dependent optical constants. The governing equations for the temporal evolution of the dust temperature and mass (or radius) were solved by the first-order explicit Euler method with automatic selection of the time step. The calculations were terminated, when the ratio of the dust radius to the initial dust radius has become less than 0.01.

B. Temporal evolution of dust temperature and mass

Figures 3(a)–3(d) show, respectively, the temporal evolutions of the tungsten dust temperature and the radius, the radiation power loss, and the emissivity for different emissivity adoptions in the uniform plasma. The plasma parameters used here are as follows: $T_e = T_i = 10$ eV, $T_a = 3.0$ eV, $n_i = n_e = n_a = 2.0 \times 10^{13}$ cm^{-3}, which are typical parameters for tokamak edge.

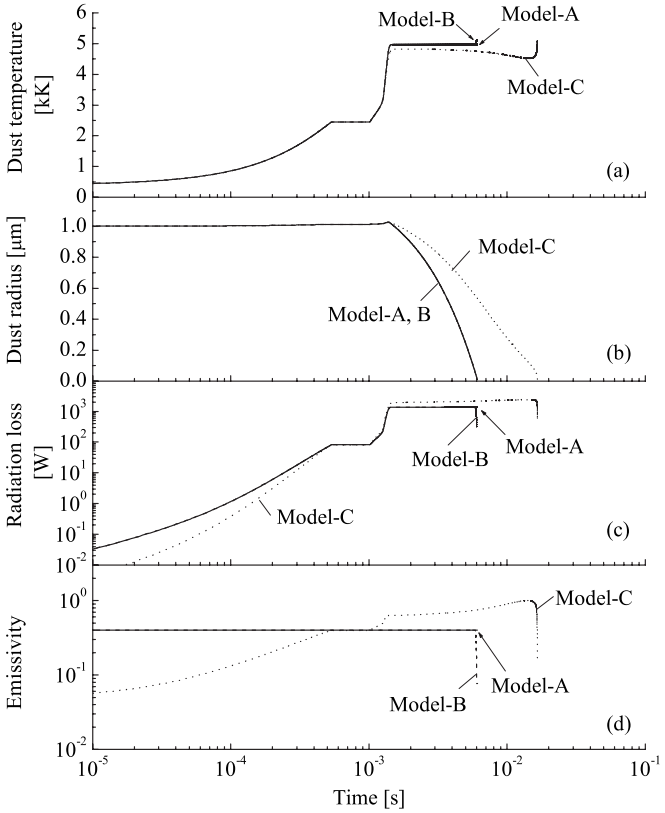

FIG. 3. Temporal evolution of (a) temperature, (b) radius, (c) radiation loss, and (d) the emissivity of the tungsten dust particle in the uniform plasma with parameters: $T_e=T_i=10$ eV, $T_a=3$ eV, $n_e=n_i=n_a=2\times10^{13}$ cm^{-3}. Initial dust radius is 1.0 μm.

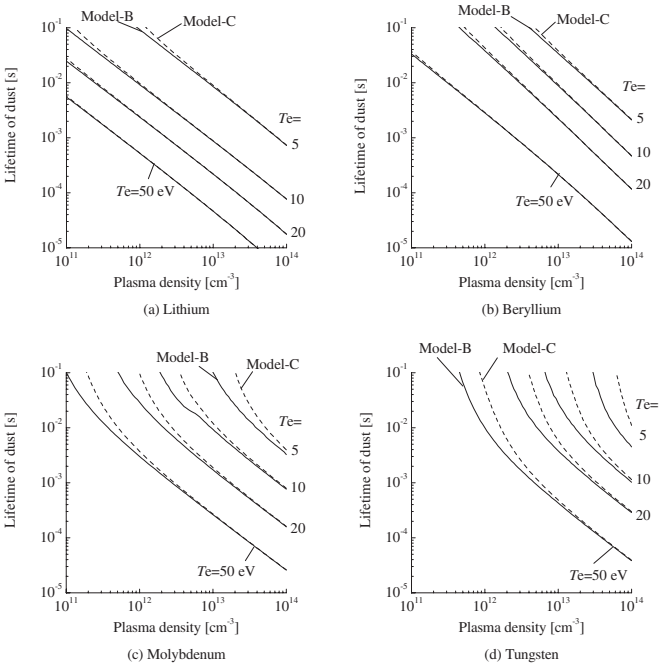

FIG. 4. Lifetime of dust particles displayed for different materials as functions of plasma density and temperature. Plasma parameters are: $T_i=T_e$, $T_a=0.3T_i$, $n_e=n_i=n_a$. Initial dust radius is 1.0 μm.

In Fig. 3, the curves "Model-A," "Model-B," and "Model-C" show results, respectively, using the constant emissivity, the emissivity with the small-body correction, and the temperature- and radius-dependent emissivity derived by Mie theory and Drude theory models for the optical constants. As can be seen, the dust temperature increases gradually up to the melting point in 0.5 ms after putting a dust particle in a uniform plasma. From $t=0.5$ to 1.0 ms, the dust temperature has a constant value of 2479 K, corresponding to the melting process of the tungsten. By the time $t=1.0$ ms, the temporal evolution of the temperature and radius hardly have differences among Models A, B, and C. This is because up to this time, the dust temperature is lower than 2500 K, where the thermal radiation loss below 2×10^2 W is not a predominant component in the energy balance of a dust particle. After that, the dust temperature rapidly increases from 1.0 to 1.5 ms, reaching to the equilibrium temperature around 4800–5000 K for evaporation.

During the evaporation process, the temperature is again almost constant, while the dust radius is rapidly decreased. In this process, there is a difference in dust temperature and radius variations among Models A, B, and C. The thermal radiation loss in Model C is higher than those in the other models Models A and B, since Model C has a higher emissivity for the present dust temperature and radius, as indicated in Fig. 3(d). As a result, the equilibrium temperature for evaporation in Model C is lower than others. At the same time, the evaporation rate is decreased, which causes slower variation in the radius. Thus, lifetime of the dust estimated by Model C becomes longer than those by the other models.

C. Lifetime of dust made of different materials

The lifetime is one important characteristic of dust particle dynamics in fusion plasmas because it is related to the ability of the dust particle to travel long distances in plasmas and to be an impurity source in various plasma regions. The lifetime for Li, Be, Mo, and W dust particles is displayed as a function of electron density n_e and electron temperature T_e in panels (a)–(d) in Fig. 4, respectively. The curves are plotted for electron density in the range of 10^{11}–10^{14} cm^{-3} and for a set of different electron temperatures in the range of 5–50 eV. These plasma parameters were used because they are typical for tokamak edge plasmas.

As seen on all panels, increasing T_e and n_e decreases the dust lifetime monotonically. This is because of the greater energy flux onto the dust for larger T_e and n_e, which increases the dust temperature and enhances the dust evaporation rate. One noticeable point in these panels is a difference in the lifetime estimated in Models B and C. Note that the lifetime calculated by Model A is almost the same to those by Model B. There is little difference in the lifetime of any of the four types of dust particles obtained by Model C or Model B for the higher values of n_e and T_e. This is attributed to the fact that the dust particle receives much higher energy flux from the surrounding plasma with higher n_e and T_e than it radiates at an evaporation temperature. On the other hand, with lower n_e and T_e, the lifetime of a dust particle by Model C is longer than that by Model B. This difference is more apparent for refractory metal dust like Mo and W. These metals have higher evaporation temperatures than light metals, which makes thermal radiation loss an important con-

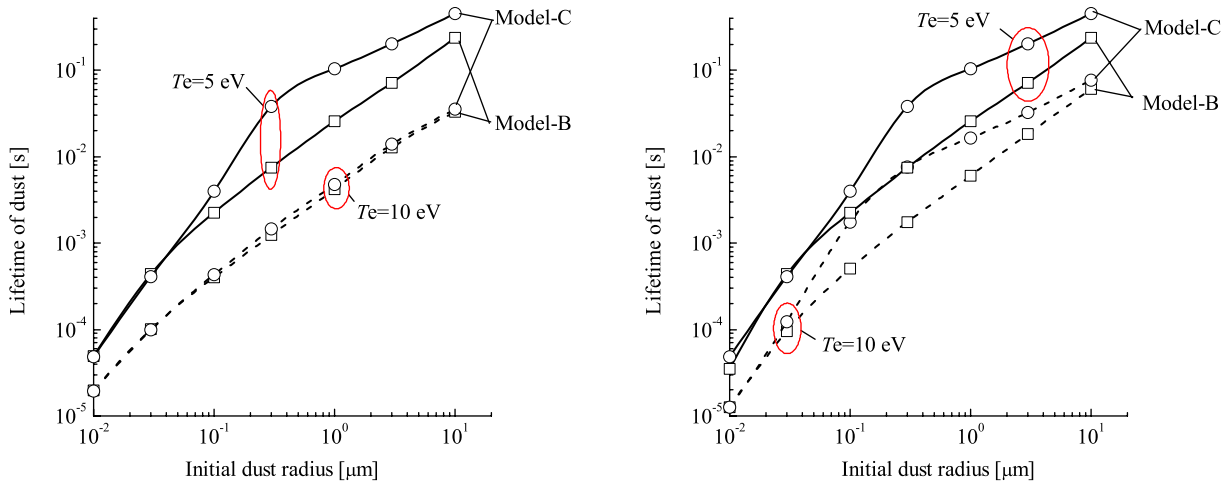

FIG. 5. (Color online) Lifetime of molybdenum and tungsten dust particles as a function of initial dust radius in two types of plasmas: solid curve indicates results with $T_i=T_e=10$ eV and $T_a=3$ eV; dotted curve is with $T_i=T_e=5$ eV and $T_a=1.5$ eV. For any cases, plasma density is fixed at 2×10^{13} cm^{-3}. (a) Molybdenum dust. (b) Tungsten dust.

tributor in the energy balance of the dust particle during evaporation process. Thus, the difference in the emissivity can lead to a large difference in the lifetime, especially in lower n_e and lower T_e plasmas.

Figures 5(a) and 5(b) show the lifetime of molybdenum and tungsten dust particles as a function of initial dust radius in two types of background plasma conditions: with $T_i=T_e=5$ eV and $T_a=1.5$ eV, as well as $T_i=T_e=10$ eV and $T_a=3$ eV. The electron density is fixed at 2×10^{13} cm^{-3}. This figure includes the calculation results of the lifetime by Model B and Model C.

When the initial dust radius is very small below 0.01 μm, the lifetime of the molybdenum and tungsten dust particles is hardly influenced by the temperature- and radius-dependent emissivity for $T_e=5$ and 10 eV, in spite of a large temperature dependence in the emissivity, as seen in Figs. 1(b) and 1(c). This slight influence of the emissivity on the dust lifetime is because the evaporation is completed in a short time for the small radius dust. On the other hand, in case that tungsten dust has a very large radius above 10 μm, its lifetime is also almost not affected by the difference in the emissivity for $T_e=10$ eV. This is because the selected value of 0.4 for the constant emissivity for tungsten dust by Models A and B is close to the emissivity of large tungsten dust at high temperatures as indicated in Fig. 1(c). For molybdenum dust in plasma with $T_e=10$ eV, the lifetime is practically independent of the adopted emissivity methods.

On the other hand, when the dust radius is in the range from 0.1 to 1.0 μm, the emissivity does influence the molybdenum dust lifetime for $T_e=5$ eV and also the tungsten dust lifetime for $T_e=5$ and 10 eV. This means that for dust with a radius of 0.01 to 10 μm, accurate emissivity is necessary to estimate lifetime adequately in plasmas with a lower electron temperature. Such a large influence of the emissivity on dust behavior with a radius of 0.01 to 10 μm results from the fact that the emissivity has a maximum for the radius around 0.1 μm at dust temperature above 2500 K in Fig. 1(c).

V. INFLUENCE OF THE EMISSIVITY ON THE DUST BEHAVIOR IN A TOKAMAK PLASMA

In many cases, dust dynamics or trajectories in some plasmas weakly depends on the emissivity. However, in some cases, a difference appears in the behavior of a heavy metal dust like a Mo and a W dust particle in low temperature or low density plasmas as seen in the previous sections. As an example, the trajectories of molybdenum dust particles were simulated in the typical edge plasma in the Alcator C-Mod tokamak. The plasma facing components of this device are made mainly from molybdenum,[43] and then a molybdenum dust particle may appear. A test molybdenum dust particle was injected from the position on the outer divertor plate toward the core plasma. The total emissivity of the molybdenum dust particle was simulated according to the Models A, B, and C to study the emissivity influence on dust behaviors.

Figure 6(a) plots the simulated three trajectories of molybdenum dust particles in the poloidal cross section of the Alcator C-Mod tokamak device using the three different emissivities by Models A, B, and C. For these calculations, the initial radius and the initial velocity of the dust particle were set to 1.0 μm and 10 m/s, respectively. The dust particle is launched toward the X-point with an initial dust temperature 400 K. The dust particle travels from the initial position toward the separatrix in the private flux region, where the electron temperature is about 3–10 eV and the ion density is about 10^{12}–10^{13} cm^{-3}. The dust particle evaporates rapidly as it approaches the separatrix. This rapid evaporation is due to the high electron and ion temperatures of more than 30 eV and the high density of 10^{14} cm^{-3} near the separatrix. As seen in this figure, there is no difference in dust trajectories with the different models for the emissivity. Similarly, from other calculations, it was found that many dust particles launched in this background C-Mod plasma hardly have different trajectories for the different emissivity

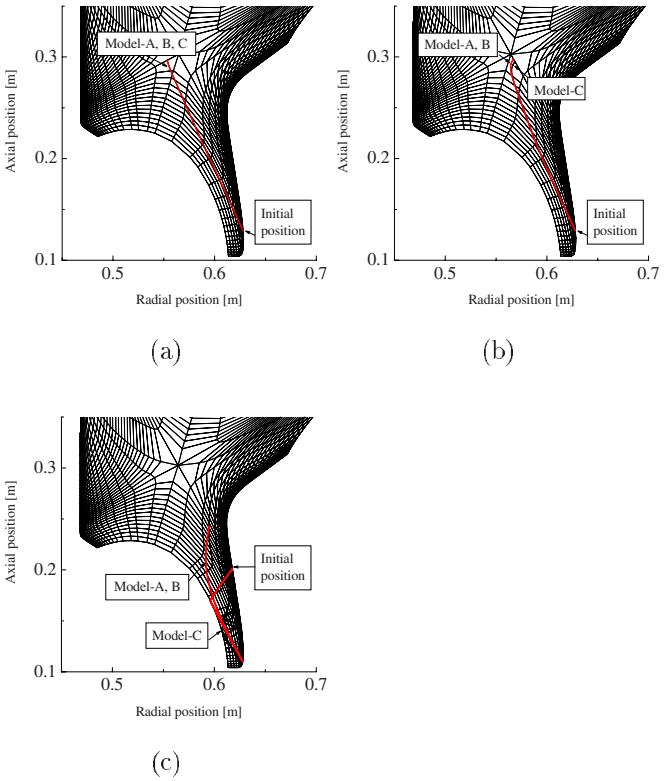

FIG. 6. (Color online) Examples of trajectories of molybdenum dust particle in the edge plasma of the Alcator C-Mod tokamak. (a) Initial radius: 1.0 μm; initial velocity: 10 m/s. (b) Initial radius: 0.12 μm, initial velocity: 28 m/s. (c) Initial radius: 1.0 μm; initial velocity: 1.0 m/s.

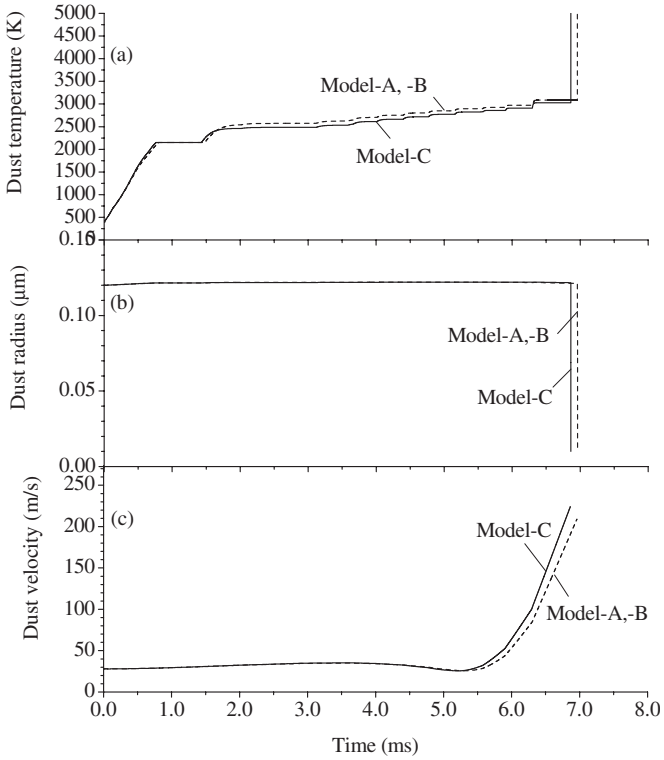

FIG. 7. Time variation in (a) dust temperature, (b) dust radius, and (c) dust velocity in the Alcator C-Mod tokamak corresponding to Fig. 6(b).

models. On the other hand, if the initial radius and initial velocity of the dust particle were set to some particular values, a difference in dust trajectories may appear even in the same background plasmas. Figure 6(b) demonstrates the three trajectories of molybdenum dust particles with an initial radius of 0.12 μm and an initial velocity of 28 m/s using the three different emissivities by Models A, B, and C, as an example. The initial position and the initial direction of the dust particle are the same as in Fig. 6(a). In Fig. 6(b), no difference is seen in the trajectories of the dust particles for the Model A and B. Neither difference is there in the trajectories by Model C against the above ones until the dust particle is close to as in the separatrix. However, near the separatrix, the dust trajectory using Model C differs from the others a little bit. The difference in the end points of the dust trajectories in this case was evaluated to be 0.332 m in three dimensions, considering a position difference not only in radial and vertical directions but also in the toroidal direction. This difference in the dust trajectories is due mainly to a difference in ion drag force acting on the dust particle from the plasma. This is because the electric charge of the dust is affected by the dust temperature which markedly changes the thermionic electron emission rate. The dust temperature is related with the emissivity through cooling rate of the dust. As a result, the dust trajectory is influenced by the emissivity of dust material.

Another rare example case in which a large difference in dust trajectory can be seen with the different emissivity models is shown in Fig. 6(c), as an example. These are the three trajectories of molybdenum dust particles launched from another position with an initial radius of 1.0 μm and an initial velocity of 1.0 m/s using the three different emissivities by Models A, B, and C. As seen, there are almost no difference in dust trajectories with Models A and B. However, the dust trajectory with Model C is much different from the others after the third reflection against the wall around the radial position of 0.63 m and the axial position of 0.11 m in the C-Mod. This large difference in the dust trajectory after a number of reflections is due to the sensitivity for the dust reflection angle against the wall, which is firstly contributed from a small difference in dust trajectories with Model B and Model C.

Figure 7 shows temporal evolution in temperature, radius, and velocity of the test molybdenum dust particles during their motion in the tokamak plasma that shown in Fig. 6(b). The temperature of the dust particles increases up to its melting temperature 2150 K that remains constant during melting from t=0.767 to 1.48 ms. The dust velocity also increases due to acceleration by ion flow in the plasma. Up to this time up to 1.48 ms, little difference is seen in dust temperature, radius, and velocity for different models adopted for the emissivity. After this time, the dust temperature again increases gradually. The rate of the temperature increase is lower in Model C than in Model A and B, since Model C adopts the higher emissivity in this temperature range. As a result, the dust temperature in Model C is a little lower than those in the other models during the heating process.

VI. CONCLUSIONS

The influence of the emissivity on the behavior of metallic dust particle (Li, Be, stainless steel, Mo, and W) was estimated by the DUSTT code. The temperature- and radius-dependent emissivity of a dust particle was calculated for different dust materials using the Mie theory and temperature-dependent optical constant model (see Ref. 25). The temporal evolution of the dust temperature and dust radius was calculated for a uniform plasma condition. For a dust particle composed of Mo or W with higher evaporation temperature, the emissivity can influence the temporal evolution of the dust temperature and then the evaporation rate because the thermal radiation is an important dust cooling mechanism at high temperature above 2500 K. The lifetime of the dust was also estimated for different materials as function of plasma parameters. It was shown that the emissivity influences the lifetime of the refractive metallic dust particle more as the plasma density and temperature decreases The influence of the emissivity on dynamics of dust particles in nonuniform tokamak plasmas was also presented. In many cases it hardly affects dynamics of the dust particle. However, in some cases the dynamics of a heavy metallic dust particle can be influenced by the emissivity. This is because the thermal radiation energy loss can be significant for a dust with temperatures above 2500 K. The presented results can be useful for estimates of penetration length of dust particles made of different materials traveling in fusion devices.

ACKNOWLEDGMENTS

One of the authors (Y.T.) would like to express his appreciation to Professor Y. Uesugi, Kanazawa University, for his advice. This work was supported in part by the USDOE Grant No. DE-FG02-04ER54852.

[1] A. Yu. Pigarov, S. I. Krasheninnikov, T. K. Soboleva, and T. D. Rognlien, Phys. Plasmas **12**, 122508 (2005).
[2] A. Yu. Pigarov, R. D. Smirnov, S. I. Krasheninnikov, T. D. Rognlien, M. Rosenberg, and T. K. Soboleva, J. Nucl. Mater. **363–365**, 216 (2007).
[3] R. D. Smirnov, A. Y. Pigarov, M. Rosenberg, S. I. Krasheninnikov, and D. A. Mendis, Plasma Phys. Controlled Fusion **49**, 347 (2007).
[4] S. I. Krasheninnikov, Y. Tomita, R. D. Smirnov, and R. K. Janev, Phys. Plasmas **11**, 3141 (2004).
[5] S. I. Krasheninnikov and T. K. Soboleva, Plasma Phys. Controlled Fusion **47**, A339 (2005).
[6] S. I. Krasheninnikov, A. Yu. Pigarov, Y. Tanaka, I. H. Hutchinson, T. D. Rognlien, and T. K. Soboleva, Contrib. Plasma Phys. **46**, 611 (2006).
[7] S. I. Krasheninnikov, L. E. Zakharov, and G. V. Pereverzev, Phys. Plasmas **10**, 1678 (2003).
[8] R. E. Nygren, D. F. Cowgill, M. A. Ulrickson, B. E. Nelson, P. J. Fogarty, T. D. Rognlien, M. E. Rensink, A. Hassanein, S. S. Smolentsev, and M. Kotschenreuther, Fusion Eng. Des. **72**, 223 (2004).
[9] T. D. Rognlien, J. L. Milovich, M. E. Rensink, and G. D. Porter, J. Nucl. Mater. **196–198**, 347 (1992).
[10] A. Yu. Pigarov, E. M. Hollmann, S. I. Krasheninnikov, T. D. Rognlien, and W. P. West, J. Nucl. Mater. **337–339**, 371 (2005).
[11] A. Yu. Pigarov, S. I. Krasheninnikov, and B. LaBombard, Contrib. Plasma Phys. **46**, 604 (2006).
[12] J. Winter, Plasma Phys. Controlled Fusion **46**, B583 (2004).
[13] A. L. Roquemore, W. Davis, R. Kaita, C. H. Skinner, R. Maqueda, and N. Nishino, Rev. Sci. Instrum. **77**, 10E526 (2006).
[14] A. L. Roquemore, N. Nishino, C. H. Skinner, C. Bush, R. Kaita, R. Maqueda, A. Yu. Pigarov, and S. I. Krasheninnikov, J. Nucl. Mater. **363–365**, 222 (2007).
[15] M. Rubel, M. Cecconello, J. A. Malmberg, G. Sergienko, W. Biel, J. R. Drake, A. Hedqvist, A. Huber, and V. Philipps, Nucl. Fusion **41**, 1087 (2001).
[16] L. A. Dorf, A. L. Roquemore, G. A. Wurden, C. M. Ticos, and Z. Wang, Rev. Sci. Instrum. **77**, 10E517 (2006).
[17] J. Winter and G. Gebauer, J. Nucl. Mater. **266–269**, 228 (1999).
[18] G. Federici, C. H. Skinner, J. N. Brooks, J. P. Coad, C. Grisolia, A. A. Haasz, A. Hassanein, V. Philipps, C. S. Pitcher, J. Roth, W. R. Wampler, and D. G. Whyte, Nucl. Fusion **41**, 1967 (2001).
[19] S. Takamura, N. Ohno, D. Nishijima, and Y. Uesugi, Plasma Sources Sci. Technol. **11**, A42 (2002).
[20] N. Ohno, Y. Kobayashi, T. Sugimoto, and S. Takamura, J. Nucl. Mater. **337–339**, 35 (2005).
[21] J. P. Sharpe, P. W. Humrickhouse, C. H. Skinner, the NSTX Team, T. Tanabe, K. Masaki, N. Miya, the JT-60U Team, and A. Sagara, J. Nucl. Mater. **337–339**, 1000 (2005).
[22] Z. Wang and G. A. Wurden, Rev. Sci. Instrum. **74**, 1887 (2003).
[23] C. M. Ticos, Z. H. Wang, G. L. Delzanno, and G. Lapenta, Phys. Plasmas **13**, 103501 (2006).
[24] Y. Tanaka, A. Yu. Pigarov, R. D. Smirnov, S. I. Krasheninnikov, N. Ohno, and Y. Uesugi, Phys. Plasmas **14**, 052504 (2007).
[25] M. Rosenberg, R. D. Smirnov, and A. Yu. Pigarov, J. Phys. D **41**, 015202 (2008).
[26] W. T. Doyle, Phys. Rev. B **39**, 9852 (1989).
[27] G. Mie, Ann. Phys. **25**, 377 (1908).
[28] P. Drude, Ann. Phys. **1**, 556 (1900).
[29] M. A. Ordal, L. L. Long, R. J. Bell, S. E. Bell, R. R. Bell, R. W. Alexander, and C. A. Ward, Appl. Opt. **22**, 1099 (1983).
[30] M. A. Ordal, R. J. Bell, R. W. Alexander Jr., L. L. Long, and M. R. Querry, Appl. Opt. **24**, 4493 (1985).
[31] G. S. Arnold, Appl. Opt. **23**, 1434 (1984).
[32] M. Rosenberg, R. D. Smirnov, and A. Yu. Pigarov, "A note on thermal radiation from fusion related metals," submitted to Fusion Eng. Des.
[33] R. Siegel and J. R. Howell, *Thermal Radiation Heat Transfer*, 2nd ed. (Hemisphere, Washington, DC, 1981), Appendix D.
[34] Y. Tanaka, T. Muroya, K. Hayashi, and Y. Uesugi, IEEE Trans. Plasma Sci. **35**, 197 (2007).
[35] Y. Tanaka, Y. Takeuchi, T. Sakuyama, Y. Uesugi, S. Kaneko, and S. Okabe, J. Phys. D **41**, 025203 (2008).
[36] C. F. Boheren and D. R. Huffman, *Absorption and Scattering of Light by Small Particles* (John Wiley & Sons, New York.1983).
[37] P. D. Desai, T. K. Chu, H. M. James, and C. Y. Ho, J. Phys. Chem. Ref. Data **13**, 1069 (1984).
[38] T. C. Chi, J. Phys. Chem. Ref. Data **8**, 439 (1979).
[39] M. Boivineau, L. Arles, J. M. Vermeulen, and Th. Thevenin, Int. J. Thermophys. **14**, 427 (1993).
[40] A. D. Rakic, A. B. Djurisic, J. M. Elazar, and M. L. Majewski, Appl. Opt. **37**, 5271 (1998).
[41] W. J. Wiscombe, Appl. Opt. **19**, 1505 (1980).
[42] Yu. V. Martynenko and L. I. Ognev, Tech. Phys. **50**, 1522 (2005).
[43] I. H. Hutchinson, R. Boivin, F. Bombarda, P. Bonoli, S. Fairfax, C. Fiore, J. Goetz, S. Golovato, R. Granetz, and M. Greenwald, Phys. Plasmas **1**, 1511 (1994).